MACHINABILITY OF DUCTILE SINGLE-PHASE MATERIALS USED IN ACCELERATOR COMPONENTS
- A STUDY WITH FOCUS ON SURFACE INTEGRITY

M. Olsson, A. Andersson, F. Schultheiss, V. Bushlya, J.-E. Ståhl

Lund University, Division of Production and Materials Engineering, Lund, Sweden

mike.olsson@iprod.lth.se

Abstract: The focus of this article has been to analyse the machinability, with focus on surface integrity, of oxygen-free copper (OFC) and niobium during turning operations. The results from machining OFC proved that all of the tools that was tested can be used to achieve a surface roughness below R_a = 0.8 µm with the correct cutting data. From the results when machining niobium it showed that only the cemented carbide tool with a nose radius of 1.2 mm was able to achieve a surface roughness of R_a = 0.8 µm or greater. The cutting resistance based on the measured cutting forces was high for both of the materials.

Keywords: Oxygen-free copper, niobium, metal cutting

1. INTRODUCTION

There are now two big science infrastructure projects under construction or at the final planning stages in Lund, Sweden. MAX IV is a synchrotron light source which accelerates electrons to produce light, it is a national project where construction was started in 2010 Max IV, (2014). The second big science infrastructure project is the European Spallation Source (ESS) which is an international neutron spallation facility that is in the final stages of planning. ESS accelerates protons that hit a target material of tungsten which produces neutrons in a spallation process ESS, (2014). A particle accelerator consists of a large number of different components which, among other things, usually includes one or several acceleration cavities. A cavity is a complex and essential part in the acceleration process. A cavity is usually made of oxygen-free copper (OFC) due to the high electrical and thermal conductivities or niobium for the superconducting effect according to Proch, (1997), which is of importance in the acceleration process. The public knowledge about machining of ductile single-phase materials such as these has thus far been limited. Many of the components produced to a particle accelerator have high requirements on surface roughness and tolerances in addition to those placed on material purity. A first step towards investigating the machinability of these materials was through performing a set of machining experiments in a laboratory environment. Questions to be addressed were what kind of problems that might occur during the machining process and which cutting data and tools that should be used to attain the sought for product quality.

2. RESEARCH METHOD

To get a better understanding about OFC and niobium material in general and especially how to machine these materials an extensive literature study was performed. Only a few scientific articles and literature were found that brought up how to machine these materials. Information about different machining operations in copper and its alloys can be found in (Copper Development Association, (1992); Davis, (2001); Nordic Brass, (2000)) here one can also find information about which tools and cutting data to be used. Niobium is used to fabricate superconducting cavities, Bauer, (1980), describes different techniques to fabricate cavities in niobium including machining of niobium. Niobium corrosive resistance have been studied by (Graham and Sutherlin), they also described different manufacturing techniques for niobium. Different manufacturing methods of niobium are also

described by ESPI Metals, (2014). Study visits were also made to the HIE-Isolde facilities at CERN and to the Maxlab facilities in Lund to gain a better knowledge about acceleration modules and its components. Interviews were performed with employees at Maxlab, Lund University and a manufacturing company to get a better understanding of the functionality of a particle accelerator and what kind of problems that might occur when manufacturing components in the investigated materials.

The machinability of a material can be defined by the upcoming tool wear, energy consumption, surface integrity, chip formation, environmental factors or a combination of these criterias according to Ståhl, (2012). The focus of the performed experiments has been to measure the attained cutting forces and surface roughness. During the experiments conducted the cutting forces were measured to be able to calculate the cutting resistance for each of the materials. Cutting resistance is a measurement to get a partly better understanding of the machinability of a workpiece material. A material with lower cutting resistance is in general easier to machine. During all the conducted experiments the attained surface roughness was measured in order to see if it is possible to achieve required surface roughnesses that have to be met when producing an accelerator cavity to HIE-ISOLDE.

The selection of cutting data and tools that were used during these experiments were based on the previously performed literature studies for both of the materials.

3. METAL CUTTING

3.1. Cutting forces

Cutting forces will arise when material gets cut away from the workpiece during a cutting process. These cutting forces can be divided into three force composants F_c, F_f and F_p. F_c is the main cutting force acting in the tangential direction to the workpiece. F_f is the cutting force acting in the feed direction, in other words the axial direction of the workpiece and occurs when the insert is moving forward in the feed direction. F_p is the so called passive cutting force pointing towards the centre of the workpiece in the radial direction. This occurs because the insert is being pushed towards the centre of the workpiece in order to attain the desired depth of cut during turning.

3.2. Cutting resistance

Knowledge about the value of the cutting resistance is a good start to evaluate the machinability of a workpiece material. Calculation of the cutting resistance includes three parameters that need to be defined. Main cutting force $F_{c,}$ the theoretical chip thickness h_1 and theoretical chip width b_1 is also required, as defined in Equation 1. Theoretical chip width b_1 and theoretical chip thickness h_1 is defined in Equation 2 and Equation 3, where a_p is the depth of cut, κ is the major cutting edge angle and f is the feed.

$$Cr = \frac{F_C}{h_1 \cdot b_1} \qquad (1) \qquad b_1 \approx \frac{a_p}{\sin\kappa} \qquad (2) \qquad h_1 \approx f \cdot \sin\kappa \qquad (3)$$

The definition of the cutting resistance is the required main cutting force per chip area when cutting the workpiece material. The cutting resistance Cr is defined in accordance with Equation 3, Ståhl (2012).

3.3. Surface roughness

The surface roughness describes the smoothness of the surface and the theoretical surface roughness is the best possible surface roughness that can be achieved. The theoretical surface roughness depends on the nose of the insert and the feed when it comes to turning operations. The arithmetic measured surface roughness R_a is defined in accordance to Equation 4 as defined in an international standard ISO 4287:1997, (1997) and is used to describe the deviation of a surface in relation to a certain mean level. Where L_m is the measured length and y is an arbitrary coordinate.

$$R_a = \frac{1}{L_m} \cdot \int_0^{L_m} |y| \cdot dx \qquad (4)$$

The derivation from Ståhl, *et al*. (2011) provides Equation 5, which is used to calculate the theoretical surface roughness, R_a. Where f is the feed and r is the nose radius of the tool. Tools with a wiper appearance can improve the surface roughness of the workpiece since it has wiper radii adjacent that increases the contact length with the workpiece. Increased surface roughness is better shown at higher feeds.

Fundamental metal cutting research has been performed by Schultheiss et al. (2014) about the connections between obtained surface integrity and the material properties of the workpiece. The ultimate yield strength and the deformation hardening are the material properties that have the most significant impact on the achieved surface integrity. The focus of this study is the selection of cutting data's influence on the surface integrity.

$$R_a \approx 0.77 \cdot \left[1 - \frac{\frac{f}{2 \cdot r}}{\arcsin\left(\frac{f}{2 \cdot r} \right)} \right] \cdot r \qquad (5)$$

4. POLAR DIAGRAM PROPERTIES

The potential machinability of a workpiece material depends on different factors such as mechanical properties, physical properties, microstructure and inclusions as previously published by (Andersson and Ståhl (2007); Xu, et al. (2013)). There are several different material properties that influence the potential machinability of a material but when making a similar polar diagram, as Andersson and Ståhl, the five parameters listed below will only be considered. This because of the selected properties is considered to have a large influence on the machinability during the metal cutting process. However there exists other properties that influence on the machinability of a material but they will not be considered in this article, (Andersson and Ståhl (2007). A polar diagram is used as a tool to compare different materials and their machinability. A known material and its material properties are used as a reference and set to the value five. The properties from the other materials are then compared to the reference material and if the polar diagrams have similar appearance one can draw the conclusion that the materials have similar machinability.

Strain hardening – affects a materials chip-producing properties during metal cutting. A high strain-hardening value means a higher energy being required for chip formation which requires higher specific cutting forces. The hardness of the machined surface will increase after machining. Strain-hardening S_n is defined according to Equation 6. The ultimate tensile strength is designated as σ_{UTS} and yield strength as σ_Y

$$s_n = \frac{R_M}{R_{p0.2}} = \frac{\sigma_{UTS}}{\sigma_Y} \qquad (6)$$

Ductility – can be defined as how much plastic deformation a material can withstand without breaking. A material with high ductility has shown high adhesion of material from the workpiece on the cutting tool during the cutting process. Materials with high ductility also have increased difficulties related to chip breakage generally resulting in longer chips.

Thermal conductivity – has an influence on the process temperature. Heat is generated by plastic deformation or friction during metal cutting and if the material has a high thermal conductivity the heat will be conducted more rapidly away from the cutting zone. High temperatures of the workpiece can have negative effects on the surface integrity and dimensional tolerances it may also cause excessive wear on the cutting tool.

Hardness – have a strong correlation with the deformation resistance and cutting resistance of a material during the metal cutting process. In general a low hardness value is favourable but in cases with materials with a high ductility it is sometimes better with a high hardness value to avoid built-up edges, burr formation and shortening of the tool life.

Abrasiveness – may have a strong negative impact on the tool life. The micro hardness can vary substantially depending on the position of the hardness measurement in the material. Enclosures of hard particles such as oxides or carbides in the workpiece material commonly have an abrasive wear effect on the tool. The abrasiveness can be calculated by using Equation 7 according to Ståhl, (2012). HV_{mean} is the mean value of the measured micro hardness values. HV_{95konf} and HV_{5konf} correspond to the 95th highest and the 5th lowest value in series of one hundred measured points. These measurements should be performed in a matrix, 10 by 10 measurements in size, in order to obtain reliable and consistent results for each material.

$$Ab = HV_{meanl} + HV_{95konf} - HV_{5konf} \qquad (7)$$

Equation 8 is used for calculating the relative value for ductility, strain hardening, hardness and abrasiveness compared to the reference material according to Xu, et al. (2013). X is the measured value for the material property in question, R is the equivalent value of the reference material property. G_{min} and G_{max} correspond to the minimum and maximum value in the interval of the evaluated material property.

$$M_x = 5 + 5 \cdot \frac{X - R}{R - G_{\min}} \rightarrow X < R \qquad M_x = 5 + 5 \cdot \frac{X - R}{G_{\max} - R} \rightarrow X > R \qquad (8)$$

Equation 9 is used when calculating the relative value for thermal conductivity. A high value on the thermal conductivity is favourable when machining a material in contrast to the other four properties whereas a lower value is desirable in most cases. The reason for having a different formula when calculating the thermal conductivity is because of a lower relative value on the thermal conductivity has a positive effect on the machinability.

$$M_x = 5 + 5 \cdot \frac{R - X}{R - G_{\min}} \rightarrow X < R \qquad M_x = 5 + 5 \cdot \frac{R - X}{G_{\max} - R} \rightarrow X > R \qquad (9)$$

Selected mechanical and physical properties are presented in Table 1 for reference material aluminium, OFC and niobium. Calculated relative values are presented in Table 2.

Table 1. Mechanical and physical properties of OFC, niobium and aluminium CES EduPack (2013).

Designation	Hardness (HV)	Abrasiveness	Ductility (%)	Strain hardening	Thermal Conductivity (W/mK)
OFC	50	3.24	49	3.67	394
Niobium	85	-	33	6.56	56
Aluminium	100	-	8	1.17	172

Table 2. Calculated relative values of OFC, niobium and aluminium.

	Reference Aluminium	OFC	Niobium
Factor	Relative value	Relative value	Relative value
Hardness	5	1.43	2.74
Abrasiveness	5	5.46	5
Ductility	5	8.94	7.5
Strain hardening	5	9.41	6.56
Thermal Conductivity	5	1.01	8.02

5. EXPERIMENTAL STUDIES

OFC with 99.99 wt. % Cu and niobium with 99.7 wt. % Nb were experimentally evaluated. A NC-controlled lathe was used for the turning experiments. The attained cutting forces were measured with a piezoelectric Kistler 9129-AA cutting force sensor. A MahrSurf PS1 was used to measure the surface roughness. The machine uses a needle that travels a specified length to collect a number of measurements, attained result is an average of the measured points. Three different tools were used during the OFC experiments; uncoated carbide (HMO) CNMG120408 both with and without a wiper (Wiper) CNMG120408W and diamond tools (PCD) CCMW120408F were also tested. For the niobium experiments uncoated cemented carbide was used. Three different nose radiuses were used 0.4, 0.8 and 1.2 mm for a CNMG1204XX tool geometry (HMU).

The machining experiment first performed was to incrementally increase the feed during longitudinal turning while both depth of cut and cutting speed remained constant during which the attained cutting forces were measured and later analysed. In a second experiment surface roughness during different cutting data while longitudinal turning both OFC and niobium was measured. For the case of turning OFC both the cutting speed and feed were varied while the depth of cut remained constant. Based on findings in the conducted literature study (Bauer, (1980), (Graham and Sutherlin) and ESPI Metals, (2014)) were the recommended cutting speed for cemented carbide tools varied in a small range between 60-90 (m/min) and the feed between 0.01-0.3 (mm/rev), it was decided that only the feed was a variable parameter during these experiments. The cutting data used was

based on the cutting data attained from the literature studies. Tests with a constant feed of 0.1 (mm/rev) and variations in cutting speeds of 20-200 (m/min) were performed for niobium to evaluate the optimal cutting speed for surface roughness measurements. The cutting data that was used during the copper surface roughness experiments is listed in Table 3 and for niobium in Table 4. The major cutting edge angle κ was kept constant to 95° during all experiments. During the performed experiments of incrementally increasing the feed for copper, the cutting speed was set to 200 m/min at a depth of cut of 2.5 mm while the feed varied between 0.05-0.50 mm/rev. For the niobium experiments the cutting speed was set to 100 m/min at a depth of cut of 2.5 mm while the feed varied between 0.02-0.40 mm/rev.

Table 3. Cutting data OFC.

Tool	Cutting speed (m/min)	Feed (mm/rev)	Cutting depth (mm)
HMO/Wiper	90-240	0.05-0.4	0.5
PCD	300-800	0.05-0.2	0.2

Table 4. Cutting data Niobium.

Tool radius (mm)	Cutting speed (m/min)	Feed (mm/rev)	Cutting depth (mm)
0.4	120	0.05-0.125	1.5
0.8 and 1.2	120	0.05-0.4	1.5

6. RESULTS AND DISCUSSION

6.1. Cutting resistance

From the measured cutting forces for the HMO tool, the cutting resistance for the OFC and niobium was calculated. Aluminium was used as a reference material in this case in order to aid the comparison. The cutting resistance for OFC and the reference material aluminium is shown in Fig 1. In this graph it is possible to see that the cutting resistance for OFC is substantially higher than that for aluminium. The calculated cutting resistance as based on the experimentally measured cutting forces for niobium is shown in Fig 2. Compared to the OFC the cutting resistance is significantly higher for niobium. Both copper and niobium are comparatively ductile materials as compared to for instance ordinary steels which make them difficult to machine.

During the experiments a burr formation was noticed in front of the tool which implied that the tool pushed a ring of material in front of itself through plastically deforming the workpiece material during the experiments. The burr formation consists of material that has not yet been cut in the machining process but instead builds up to an extra ridge of material in front of the tool. This burr formation is believed to be one of the explanations for the high cutting resistance of the materials as compared to aluminium, Fig 1. A high cutting resistance was attained for both materials as compared to other more common materials like aluminium. A theory on why this occurs is probably a phenomenon that could be compared to as if there was an increased a_p. During the cutting process the depth of cut a_p was found to increase with an extra depth ofcut a_p* due to the burr formation that the tool pushes ahead of itself. This results in a higher main cutting force which in turn leads to a larger cutting resistance value because of the additional a_p* which will not normally be taken into account while calculating C_r, see Fig 3. The arrows in Fig 3 indicates the material flow that creates a burr formation which results in an increased cutting depth a_p*.

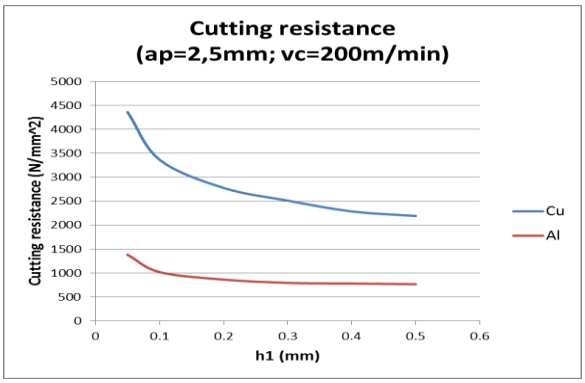

Fig. 1. Cutting resistance OFC compared to aluminium

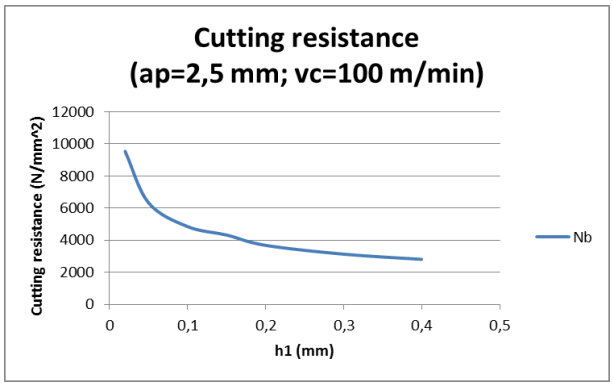

Fig. 2. Cutting resistance niobium.

6.2. Surface roughness

In Fig 4, the measured R_a surface roughness is shown as a function of the feed for the HMO tool at four different cutting speeds. This is plotted against the calculated theoretical surface roughness according to Equation 5. In the Fig 4 it is possible to observe that the measured Ra surface roughnesses are numerically almost the same as the theoretical surface roughness at low feeds for the HMO tool. With increased feed the measured surface roughnesses are however lower than expected theoretical values. When comparing the surface roughness attained for the HMO and Wiper tools, the HMO tools showed better results through a decreased Ra surface

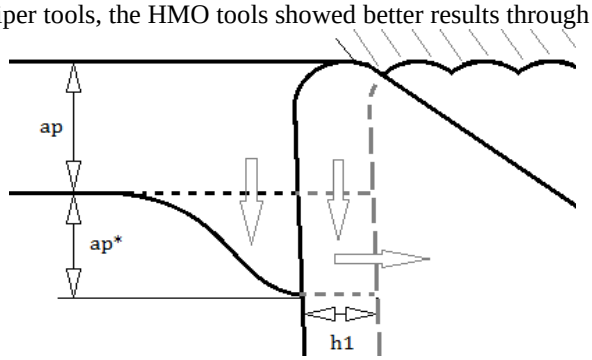

Fig. 3. Increased depth of cut a_p.

roughness value at a lower cutting speed. When the feed was increased to 0.15 mm/rev and above the wiper showed better results for higher speeds compared to the HMO tool which was expected, see Fig 4 and Fig 5.

When cutting with the PCD tool the best obtained results was when cutting with lower feeds between 0.05-0.15 mm/rev and speeds between 300-600 m/min, see Fig 6. Problems with re-weld, hot chips sticking on the machined surface of the material seemed to be lower than for the other tools.

The HMU tools with nose radii of 0.4 and 0.8 mm showed substantial variation of the measured R_a-values when performing these surface roughness experiments, see Fig 7 and Fig 8. All the measured R_a-values are plotted and the continuous line plotted is an average value of all the measured R_a-values. This is plotted against the theoretical calculated R_a surface roughness. As anticipated better results were obtained, as of decreased

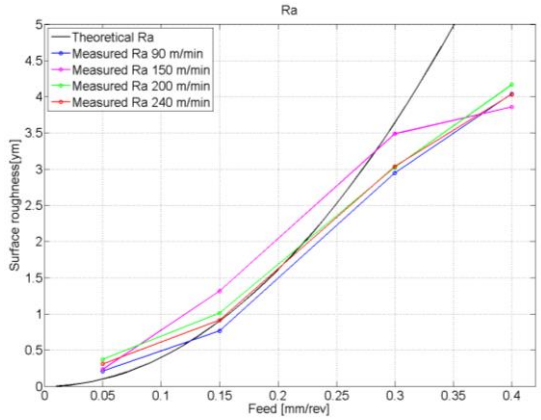

Fig. 4. Surface roughness HMO tool.

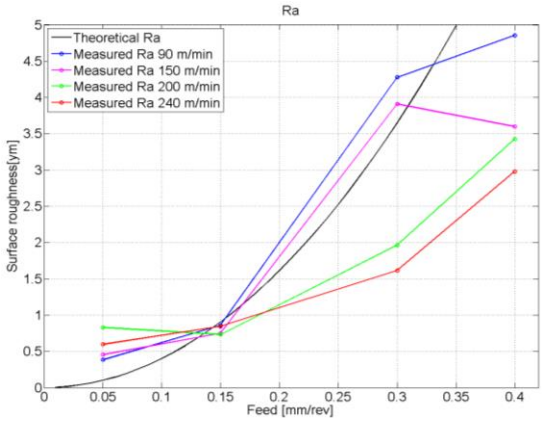

Fig. 5. Surface roughness Wiper tool.

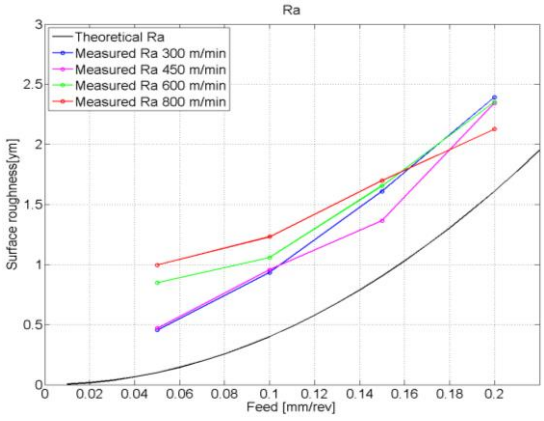

Fig. 6. Surface roughness PCD tool.

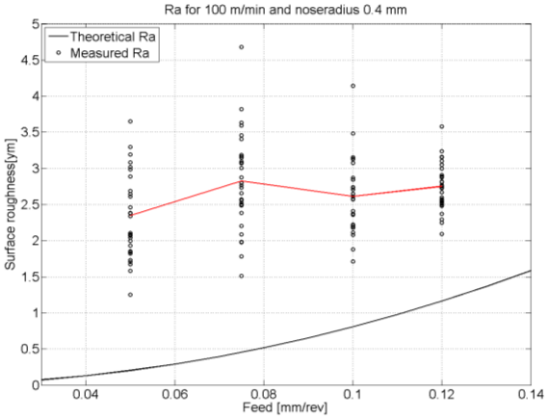

Fig. 7. Surface finish nose radius 0.4 mm.

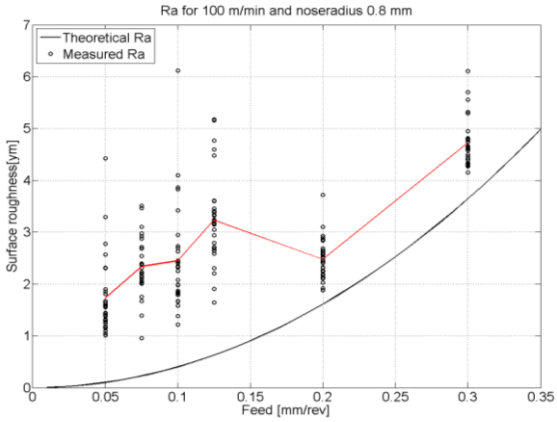

Fig. 8. Surface finish nose radius 0.8 mm

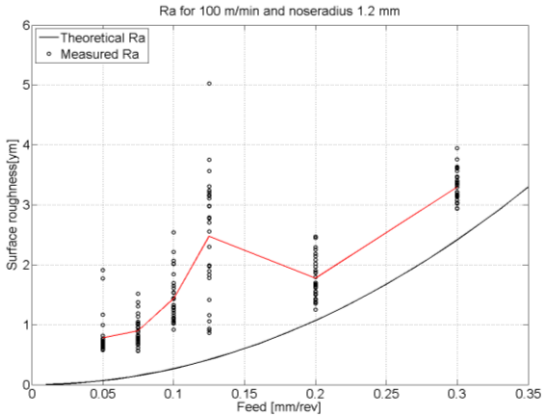

Fig. 9. Surface finish nose radius 1.2 mm.

measured R_a-values with the HMU tool that had a 1.2 mm nose radius compared to the HMU tools with a smaller nose radius. The measured R_a-values do not vary as much as for the other two tools while turning niobium and the measured R_a-values are closer to the theoretical expected values, see Fig 9. The lowest average R_a-value achieved was 0.78 µm at a feed of 0.05 mm/rev. In general niobium proved to be a difficult material to machine with bad surface roughness as a result this due to continuous chips, burr formation and re-weld of chips on the surface. This can explain the wide range of the measured surface roughness points.

6.3. Polar diagram

The polar machinability diagram in Fig 10 shows similar values on the different axes for OFC and niobium. The biggest difference is for the thermal conductivity, niobium has a low thermal conductivity compared to OFC which is undesirable during metal cutting. Both OFC and niobium have low hardness value compared to more

common machining steel for example C45E/SS 1672, this could be positive but if the materials also have a high ductility it could lead to a more difficult material to machine. Problems with longer chips or difficulties with cutting off the material from the workpiece can occur. The abrasiveness for niobium has not yet been determined by measurements, the value was set to five as for the reference material.

7. CONCLUSIONS

Based on the results from the conducted experiments, conclusions can be made that both OFC and niobium are unpredictable materials when machining due to the significant variations of the attained surface roughness. At one stage everything seems normal and the attained surface roughness is satisfactory but a moment later major problems can arise with re-welded workpiece material and an unsatisfactory surface roughness. This could potentially be due to the ductility of the workpiece materials, copper is a ductile and soft material, especially OFC, and similar things could also be said about niobium. Another big problem while machining these materials is the chip formation as commonly continuous chips are obtained. When machining the investigated materials the attained chips were continuous and the chip breakers employed on the tools seemed to have no significant effect. Problems with the chip formation also affect the surface roughness because the chips can start to tangle

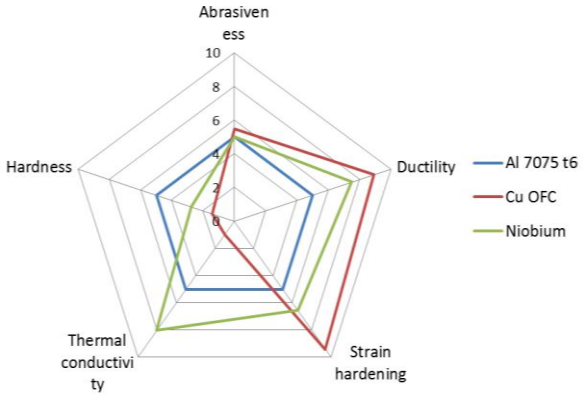

Fig. 10. Polar machinability diagram of OFC, niobium and aluminium.

around the tool or the workpiece and damage the machined surface. From the results attained during the experiments while machining OFC the drawn is that uncoated carbide, both with and without wiper, appears to produce the best results through lowering the R_a surface roughness value. When comparing the results from Fig 4 and Fig 5 the conclusion is that HMO tool should be used at lower cutting speeds and Wiper at higher. As expected the wiper geometry shows better results regarding surface roughness at higher feeds compared to conventional tools. It doesn't seem that chip breakers on the tool have any significant effect. Instead, a tool with no chip breaker like the PCD tool, have less problems with re-weld and seems to transport the chips away from the workpiece as good or even better than the other tools. The PCD tool can be used for finishing operations with small depths of cut and higher cutting speeds.

The results from the niobium experiments show that only the tool with a nose radius of 1.2 mm has satisfying R_a surface roughness results with less adhesion of chips on the surface compared to the other two tools. Better results, as of improved surface roughness, was expected with the tool that had a bigger nose radius since the contact length of the tool increases. But still the obtained results show that it is very difficult to machine niobium and more extensive experiments with different tools should be performed before any recommendations could be given according to which tools and cutting data to use when machining niobium.

8. ACKNOWLEDGEMENT

The author wish to acknowledge the Vinnova financed program SIO: **Production**2030. The author would also like to thank SECO Tools for their assistance during this study.

9. REFERENCES

Andersson, M. and J.-E. Ståhl (2007). Polar Diagram Machinability Diagram - A Model to Predict the Machinability of a Work Material. *Proceedings of the Swedish Production Symposium 2007*, Gothenburg, Sweden.

Bauer. W. (1980). Fabrication of niob cavities, *Proceedings of SRF Workshop 1980*, pp. 271-288

CES EduPack 2013, Version 12.2.13, Granta Design Limited, Cambridge, United Kingdom.

Copper Development Association, (1992) Cost-Effective Manufacturing Machining Brass, Copper and its Alloys, *Publication TN44*.

Davis, J.R. (2001), *ASM Specialty Handbook:Copper and Copper Alloys*, pp. 264-275, ASM International, Ohio.

ESPI Metals, *Machining Niob*, Available: http://www.espimetals.com/index.php/technical-data/171-Niobium-Machining (2014-05-02).

European Spallation Source (ESS), Available: http://europeanspallationsource.se/spallation (2014-05-08).

Graham R.A., Sutherlin. R.C., Niob and niob alloys in corrosive applications. *Wah Chang*, Nebraska, USA.

ISO 4287:1997 (1997), *Geometrical Product Specifications (GPS) - Surface texture: Profile method - Terms, definitions and surface texture parameters*, International Organization for Standardization.

Max IV Laboratory, Available: https://www.maxlab.lu.se/maxiv (2014-05-05).

Nordic Brass, OutoKump, *Skärande bearbetning*, Available: http://www.nordicbrass.se/LinkClick.aspx?fileticket=QLMX1EW1bCs%3D&tabid=73&mid=410&language=sv-SE (2014-05-20).

Proch, D. (1997). Superconducting cavities for accelerators. *Rep. Prog. Phys*. **61**, pp. 431-482

Schultheiss. F, Hägglund. S, Bushlya. V, Ståhl. J-E (2014). Influence of the minimum chip thickness on the obtained surface roughness during turning operations, To be submitted to the 2nd CIRP Conference on Surface Integrity.

Ståhl J.-E., F. Schultheiss, S. Hägglund, Analytical and Experimental Determination of the Ra Surface Roughness during Turning, Procedia Engineering, 19 (2011) 349-356.

Ståhl, J-E. (2012). *Metal Cutting – Theories and models*, Division of Production and Materials Engineering, Lund University in cooperation with Seco Tools AB, Textbook, Lund/Fagersta, Sweden.

Xu, L., F. Schultheiss, M. Andersson and J.-E. Ståhl (2012). General Conception of Polar Diagrams for the Evaluation of the Potential Machinability of Workpiece Materials., *International Journal of Machining and Machinability of Materials*, **14**, pp. 24-44.